

In Silico Analysis of PTP1B Inhibitors and TLC-MS Bioautography-Based Identification of Free Radical Scavenging and α -Amylase Inhibitory Compounds from Heartwood Extract of *Pterocarpus marsupium*

Mohammad Irfan Dar, Mohammad Irfan Qureshi, Sultan Zahiruddin, Sageer Abass, Bisma Jan, Armiya Sultan, and Sayeed Ahmad*



Cite This: *ACS Omega* 2022, 7, 46156–46173

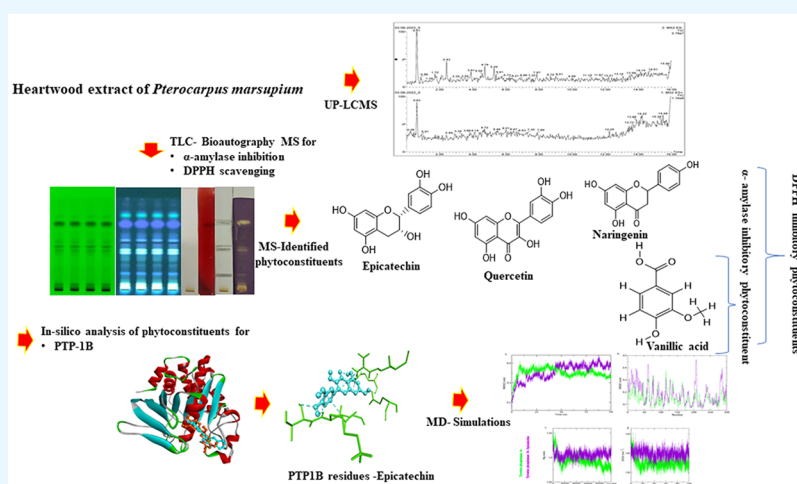


Read Online

ACCESS |

Metrics & More

Article Recommendations



ABSTRACT: Type 2 diabetes mellitus leads to metabolic impairment caused by insulin resistance and hyperglycemia, giving rise to chronic diabetic complications and poor disease prognosis. The heartwood of *Pterocarpus marsupium* has been used in Ayurveda for a long time, and we sought to find the actual mechanism(s) driving its antidiabetic potential. Methanol was used to prepare the extract using a Soxhlet extraction, and the identification of metabolites was performed by thin-layer chromatography (TLC) and ultraperformance-liquid chromatography and mass spectroscopy (UP-LCMS). The antioxidant potential of methanolic heartwood extract of *Pterocarpus marsupium* MHPM was determined using 2,2-diphenyl-1-picrylhydrazyl (DPPH) and a reducing power assay. The α -amylase and α -glucosidase enzyme inhibitory potential of MHPM were investigated for their antidiabetic activity against acarbose. TLC-MS-bioautography was performed to identify the compounds responsible for possible antioxidant and antidiabetic activities. Moreover, targeting protein tyrosine phosphatase 1B (PTP1B), a key regulator of insulin resistance, by identified metabolites from MHPM through molecular docking and all-atom molecular dynamics (MD) simulations was also undertaken, suggesting its potential as an antidiabetic herb. The IC_{50} of free-radical scavenging activity of MHPM against DPPH was $156.342 \pm 10.70 \mu\text{g/mL}$. Further, the IC_{50} values of MHPM in α -amylase and α -glucosidase enzymatic inhibitions were $158.663 \pm 10.986 \mu\text{g/mL}$ and $180.21 \pm 11.35 \mu\text{g/mL}$, respectively. TLC-MS-bioautography identified four free radical scavenging metabolites, and vanillic acid identified by MS analysis showed both free radical scavenging activity and α -amylase inhibitory activity. Among the identified metabolites from MHPM, epicatechin showed significant PTP1B docking interactions, and its MD simulations revealed that PTP1B

continued...

Received: July 7, 2022

Accepted: September 28, 2022

Published: December 9, 2022



forms a stable protein–ligand complex with epicatechin throughout the progression, which indicates that epicatechin may be used as a promising scaffold in the development of the antidiabetic drug after isolation from *Pterocarpus marsupium*. Overall, these findings imply that *Pterocarpus marsupium* is a source of valuable metabolites that are accountable for its antioxidant and antidiabetic properties.

■ INTRODUCTION

Type 2 diabetes (T2D), which is a metabolic disease largely characterized by hyperglycemia resulting from impaired insulin secretion, its action or both, leading to metabolic ailments, has currently become a global epidemic.¹ The most common form of diabetes is type 2 (T2DM), which affects approximately 90% of diabetic people. Type 1 diabetes (T1D) affects the remaining 10% of patients; this form of diabetes is caused by a lack of functioning beta cells (insulin-dependent) giving rise to insulin deficiency, whereas patients with type 2 diabetes (insulin resistance) are unable to respond to insulin, and this type can be managed with changes in diet and exercise and medicines.² T2DM has been termed as noninsulin-dependent diabetes and is the most common cause of chronic metabolic ailments, characterized by higher blood glucose levels due to the individual's poor management of insulin, which could progress to utter resistance in addition to limited β -cell activity in the long run.³ The World Health Organization's Fact Sheet on Diabetes stated that being overweight or obese is the most significant risk factor for T2DM, which is increasingly being seen in children, adolescents, and young adults. Diabetes has been expected to rise from 4% in 1995 to 5.4% by 2025, according to the report published by the World Health Organization (WHO). The WHO has forecasted that developing countries would bear the brunt of the huge numbers of cases of diabetic patients.⁴

Though the etiology of diabetes is yet unknown, scientific data suggests that the generation of free radicals or the inability to scavenge them play an important role in its progression and, more crucially, the development of diabetes-related complications. In chronic hyperglycemia, free radicals damage cellular components, DNA, peptides, and lipids, resulting in altered physiological activities⁵ and producing advanced glycation end products (AGEs), which act directly on cells and cause inflammation and oxidative stress.²

Diabetes is a complex disease with various complications associated with its progression, and it necessitates a multi-therapeutic approach. Various side effects like gastrointestinal disorders, hypoglycemia, hepatotoxicity, etc.⁵ of modern medicine treatment have prompted patients with diabetes to look for alternative treatments with fewer side effects.^{7,8} As a result of the complexity of many phytochemicals, medicinal plants are a good source of drug discovery and development. The use of medicinal plants and their derivative products has grown exponentially, as they have the fewest adverse effects. The combined effect of phytochemicals present in plants is thought to be one of the most effective and focused pharmacological therapies for restoring cellular normalcy against the harmful effects of various acute and chronic diseases. Traditional medicine uses at least 1200 varieties of plant species for their antidiabetic properties. Only a small fraction of these plant species have been scientifically investigated for their possible effect on reducing the progression of diseases, and only a few of them have had their mechanisms of action investigated.⁹

The deciduous tree *Pterocarpus marsupium* Roxb. is mostly found in Sri Lanka and India.¹⁰ It is often recognized in Hindi as Vijaysar and is an important medicinal plant used mostly in

Ayurveda to cure diabetes. Its therapeutic and laxative qualities are well-known in Ayurvedic medicine. Its blossoms are used to treat fever, its heartwood is often used as a depurative, hemostatic, and rejuvenating agent, and its wood is used to treat chest and body pain, gastritis, and other ailments.¹¹ Over centuries, the heartwood and bark of *Pterocarpus marsupium* Roxb. (PM) have been employed as an antihyperglycemic treatment.¹²

However, most studies reported on PM highlight its antidiabetic effect(s) with scarce information on its molecular mechanisms in preventing diabetic complications. In this account, we sought to pursue the antidiabetic potential and the metabolite fingerprinting of MHPM, as well as its potential in scavenging the generation of ROS. Further, the molecular mechanism of its antidiabetic potential was evaluated by *in silico* molecular approaches, highlighting epicatechin as an effective metabolite interacting with and blocking PTP1B. Further studies, however, are needed to establish epicatechin as an antidiabetic agent using suitable *in vitro* and *in vivo* models.

■ MATERIALS AND METHODS

An HPTLC system (CAMAG, Muttensz, Switzerland), TLC silica gel 60F₂₅₄ (Merck KgaA, 64271 Darmstadt, Germany), and Water's ACQUITY UPLC system (Waters Corp., MA, U.S.A.) were used for mass spectrometry analysis. A C18 column (ACQUITY UPLC BEH C18 1.7 μ m, 2.1 \times 100 mm), Mass Lynx V4.1 (Waters, U.S.A.), and HPLC water were used. α -amylase, α -glucosidase, pNPG, fast blue, 2,2-diphenyl-1-picrylhydrazyl (DPPH), quercetin, acarbose, and ascorbic acid were purchased from Sigma-Aldrich Co., St. Louis, MO, U.S.A.

Collection of Plant Material and Preparation of Plant Extract. The selected plant material was purchased from Universal Biotech (Delhi, India) and authenticated as per the standard protocol specified in the Ayurvedic Pharmacopeia of India.¹³ The authenticated plant material was disposed of at the Bioactive Natural Product Laboratory for future reference with voucher number JH/BNPL/SA/2020/PM.

Healthy heartwood of *Pterocarpus marsupium* (PM) was processed for extract preparation; the plant material was first rinsed with distilled water and was further dried in the shade for 4 to 5 days. The dried plant part was ground into a fine powder, and 50 g of the powdered sample was processed in 500 mL of methanol, at an ambient temperature of 50 °C for 6 h in the Soxhlet apparatus. Then, after cooling, the extract was filtered and the filtrate was subjected to dryness using a rotary evaporator at 40 °C under reduced pressure. The percentage yield of the extract was calculated, and the extract was stored at 4 °C for further experiments.

$$\% \text{ Yield of extract} = \left(\frac{\text{Weight of dried extract}}{\text{Weight of plant material}} \right) \times 100$$

Estimation of Total Phenolic and Flavonoid Content. The total phenol content (TPC) of MHPM was carried out by the Folin Ciocalteu method.¹⁴

The total flavonoid content (TFC) of MHPM was carried out by the aluminum chloride colorimetric method.¹⁵

In Vitro Antioxidant Activity of MHPM. The free radical scavenging potential of the MHPM was determined by 1,1-diphenyl-2-picryl-hydrazyl (DPPH) assay as per the reported protocol.¹⁶ Briefly, 0.1 mM of DPPH in 1.5 mL of DPPH solution (0.1 mM prepared in methanol) was mixed with 0.5 mL of different concentrations of MHPM (15.62–500 $\mu\text{g/mL}$). Furthermore, the reaction mixture was left in a dark place for 30 min, and finally, the absorbance of the mixture was measured at 517 nm in a UV–visible spectrophotometer (Shimadzu Corp. A116354, Japan). Ascorbic acid was used as a reference standard. The free radical scavenging activity was calculated by the following equation.

$$\{(A_0 - A_1/A_0)\} \times 100$$

where A_0 is the absorbance of the control and A_1 is the absorbance of the extracts or standard.

The % scavenging curve was plotted against the MHPM concentration, and the half maximal inhibitory concentration (IC_{50}) of the MHPM was calculated.

The reducing power of the extracts was determined by evaluating the transformation of Fe^{3+} to Fe^{2+} according to the protocol of Zahiruddin et al.¹⁷ Different concentrations of the MHPM (15.62–500 $\mu\text{g/mL}$) were mixed with 2 mL of phosphate buffer (pH 6.7) and 2 mL of potassium ferricyanide solution. The whole mixture was incubated for 30 min at 45 °C. After incubation, 2 mL of trichloroacetic acid (10%) was added to each sample, which was centrifuged for 10 min. After centrifugation, 5 mL from the upper layer of each sample was taken and mixed with 5 mL of distilled water and 1 mL of ferric chloride (0.1%). After continuous shaking, the absorbance of the solution was measured at 700 nm in a UV–visible spectrophotometer (Shimadzu Corp. A116354, Japan). The higher the absorbance, the greater the reducing power.

In Vitro Enzyme Inhibitory Activity of MHPM. α -Amylase Inhibitory Assay. α -Amylase inhibitory activity of the methanolic extract was carried out according to the reported method with minor modification.¹⁸ Briefly, 25 μL of various concentrations of MHPM or acarbose and 50 μL of α -amylase solution (4 U/mL in phosphate buffer, pH 6.7) were mixed in a 96-well plate at 37 °C and preincubated for 20 min. The mixture was again incubated at 37 °C for 30 min by adding 20 μL of starch (1% in phosphate buffer, pH 6.8). Further, 50 μL of hydrochloric acid was added to the mixture to stop the reaction, and 50 μL of iodide solution was added. The absorbance of the mixture was measured at 580 nm using a Multiplate Reader spectrophotometer (iMark Microplate Reader Bio-Rad, U.S.A.). Acarbose was used as a standard. The results were expressed as percentage inhibition, which was calculated using the formula,

$$\text{Inhibitory activity (\%)} = (1 - \text{AbT}/\text{AbC}) \times 100$$

where AbT is the absorbance in the presence of the test substance and AbC is the absorbance of the control.

α -Glucosidase Inhibitory Assay. α -Glucosidase inhibitory activity was measured according to the reported method with minor modifications.¹⁹ Briefly, a volume of 20 μL of varying concentrations of MHPM (0.1, 0.2, 0.3, 0.4, and 0.5 mg/mL) was mixed with 10 μL of α -glucosidase (1 U/mL) in a 96 well plate. The reaction mixture was preincubated at 37 °C for 15 min. The reaction mixture was again incubated at 37 °C for 20 min after adding 20 μL of *para*-nitrophenyl- α -D-glucopyranoside (5 mM) as the substrate. Further, 50 μL of sodium bicarbonate (0.1 M) was added to stop the reaction. The absorbance of the reaction mixture was measured at 405 nm

using a multiplate reader (iMark Microplate Reader Bio-Rad, U.S.A.). Acarbose at various concentrations (0.1–0.5 mg/mL) was used as the standard. The results were expressed as percentage inhibition, which was calculated using the formula,

$$\text{Inhibitory activity (\%)} = (1 - \text{AbT}/\text{AbC}) \times 100$$

where AbT is the absorbance in the presence of the test substance and AbC is the absorbance of the control.

Characterization of MHPM by TLC Profiling. TLC profiling of MHPM and the standard quercetin ($\geq 95\%$) (Sigma) was performed according to the in-house developed procedure.²⁰ An aluminum silica gel 60F254 TLC plate (5 cm \times 10 cm) was employed on which the sample and standard (4.0 μL each) were applied using a CAMAG ATS 4 syringe (Switzerland) with a delivery speed of 100 nL/s with 6.0 mm of band length. Toluene–ethyl acetate–formic acid–methanol (6:3:0.5:0.5, v/v/v/v) was used as the mobile phase. Up to 80% development/run, the plate was removed from the CAMAG twin trough glass tank and air-dried for another 10 min. Densitometric measurements were carried out in the absorbance mode at 254 and 366 nm using a CAMAG TLC Scanner 3.

TLC-MS-Bioautographic Activity. *TLC-MS Bioautography for Antioxidant Activity/DPPH Free-Radical Scavenging Activity.* TLC-bioautographic measurements of DPPH free-radical scavenging active substances were performed as per the reported method.²¹ To identify the free radical scavenging compounds in MHPM, the developed TLC plate was dipped in DPPH solution (5 mM). The yellowish band against the purple background of the plate indicated the free radical scavenging metabolites in MHPM.

TLC-MS Bioautography for α -Amylase Activity. The TLC-bioautographic-based evaluation of α -amylase active substances was carried out as per the reported method.²¹ The developed TLC plate was dipped in freshly prepared α -amylase enzyme solution (10 mg of enzyme in 20 mL of sodium acetate buffer solution) and incubated for 1.5 h in a humid desiccator. After the incubation, the plate was dipped in starch solution (1%) and again incubated for 30 min for the reaction of enzyme and substrate. Further, the plate was dipped in an iodine solution, and α -amylase inhibiting metabolites of the plate showed a dark violet color against a brown background.

Analysis of Bioactive Metabolites Isolated from TLC-Bioautography. The MS analysis of the scraped band from underivatized parallel plate having active metabolites showing free radical scavenging and α -amylase inhibitor activity was carried out on a Waters ACQUITY UPLC (TM) system (Waters Corp., MA, U.S.A.) fitted with a binary solvent delivery system, an autosampler, a column manager, and a tunable MS detector (Serial No. JAA 272; Waters, Manchester, U.K.), a triple quadrupole mass spectrometer fitted with an ESI source, installed and controlled by Mass Lynx V 4.1 (Waters, U.S.A.). For ideal chromatographic separation, acetonitrile (A) and 0.1% formic acid in water (B) were run on a uniform capillary silica-based C18 column (ACQUITY UPLC(R) BEH C18 1.7 μm , 2.1 \times 100 mm). The nebulizer gas flow was set at 500 L/h, and the cone gas flow rate was set at 50 L/h; for the cone gas, the flow was set at 50 L/h, and the supply temperature was maintained at 104 °C. The capillary and cone voltages were set at 3.0 and 40 kV, respectively. At a pressure of 5.3×10^{-5} Torr, argon was used for collision. Separated metabolites from different samples were tentatively identified using mass data sources such as Mass Bank,

PubChem, NIST Chemistry Web Book, and the literature.^{14,21,22}

Characterization of MHPM by UPLC-MS Profiling. UPLC-MS analysis can be used to identify the metabolites present in MHPM.²³ The UPLC-MS analysis of MHPM was carried out with the water's ACQUITY UPLC system (Serial No. F09 UPB 920M; Model code UPB Corp., MA, U.S.A.), equipped with a binary solvent delivery system, a column manager, an autosampler, and a tunable MS detector (Serial No. JAA 272; Synapt; Waters, Manchester, U.K.), and a triple quadrupole mass spectrometer fitted with an ESI source, installed and controlled by Mass Lynx V 4.1 (Waters, U.S.A.). Data acquisition has been done in both positive and negative modes. In gradient elution mode, the extract was chromatographically separated in a previously degassed mobile phase containing 0.5% (v/v) formic acid in water (A) and acetonitrile (B). The ACQUITYUPLCBEH C18 (100 2.1 mm 1.7 m) column was used, and the mobile phase flow velocity was 0.4 mL/min. The temperatures of the column manager and sample manager were set to 35 ± 2 °C and 25 ± 2 °C, respectively. With the help of an autoinjector, approximately 10 μ L of a sample was injected in a split mode of 5:1, and the system pressure was set to 15 000 psi. The MS detector was used to detect the separated metabolites. The nebulizer gas and cone gas flow rates were set at 500 L/h and 50 L/h, respectively. The MS detector's source temperature was set to 104 °C. Capillary and cone voltages were set to 3.0 kV and 40 kV, respectively. At a pressure of 5.3×10^{-5} Torr, argon gas was used to simulate ion collisions. Both the UPLC and the mass detector were controlled by the MassLynxV4.1 software. The separated metabolites were identified based on their *m/z* values using a mass bank and previous literature.¹⁷

In Silico Analysis of PTP1B Inhibitors. *Computational Resources.* Different bioinformatics tools, including InstaDock, Discovery Studio Visualizer, PyMOL and GROMACS,²⁴ were used for docking and simulation studies. RCSB-Protein Data Bank (PDB), the ZINC database, Swiss ADME, CarcinoPred-EL, VMD, QtGrace etc. are web resources that were employed for data retrieval and analysis. The regularized coordinates in three dimensions of protein tyrosine phosphatase (PTP-1B) were retrieved from PDB (PDB ID: 1C83). Water molecules, cocrystallized heteroatoms, and cocrystallized ligands were removed from the native coordinates. The PTP-1B structure was prepared for high-throughput screening in the Swiss PDB Viewer and InstaDock by altering missing residues, adding hydrogen atoms to polar groups, and assigning certain atom types. Potent antidiabetic phytoconstituents from UPLC-MS analysis of MHPM were selected for molecular docking; further, the most stable sample with less binding energy from docked the phytoconstituent was selected for MD simulation analysis, and its structures were retrieved from PubChem and then processed in InstaDock.

Virtual Screening Based on Molecular Docking. Molecular docking is a popular method for predicting the optimal orientation and binding affinity of biomolecules to a receptor, most commonly a protein.²⁵ Molecular docking was used to determine the optimal structure and binding affinity of the phytoconstituent toward PTP-1B. The docking was structurally blind for all the compounds with an exhaustiveness of 8, where they were free to move and search their preferential binding sites in the proteins. The protein–ligand docking was attained using InstaDock with a blind search space of a grid size of 110, 70, and 108 Å for the *X*, *Y*, and *Z* coordinates, respectively. The center of

the grid was set to *X* = 63.09, *Y* = 14.98, and *Z* = 76.91, with 1 Å grid spacing; this was suitable for housing all of the heavy atoms of PTP-1B where ligands can move quickly. Further, the docking specifications were left at their defaults. The InstaDock tool was used to determine and analyze the phytoconstituent PTP-1B binding affinities and other docking characteristics. The docking data was filtered using energy values, and then all docking poses for each phytoconstituent were created.

Molecular Simulations. MD simulations help us understand the atomic movements of proteins and protein–ligand complexes.^{26,27} MD simulation studies were used to confirm docking results of interactions between PTP-1B and the selected bioactive constituent epicatechin. The structural coordinates of the thermodynamically stable systems of free PTP-1B and its interactions with the selected compound epicatechin were authenticated by MD simulation using GROMACS v5.5.1.²⁴ The PRODRG server was used to parametrize epicatechin to generate a receptor–ligand complex topology. For solvation in the Simple Point Charge (SPC216) water model, each system was placed in the center of a cubic box with a 10 Å distance to the edges. A suitable amount of counterions (Na^+ and Cl^-) was introduced to neutralize the simulation systems. The two-step equilibration was performed for 100 ps at a fixed volume with periodic boundary settings and gradual heating from 0 K to 300 K at a pressure of 1 atm. All systems were simulated for 100 ns, and the resulting data were evaluated to determine protein–ligand stability using the GROMACS techniques.

RESULTS AND DISCUSSION

The authenticated dried heartwood of *Pterocarpus marsupium* was extracted with methanol using a Soxhlet extraction process. The percentage yield of the methanolic extract of heartwood of *Pterocarpus marsupium* (MHPM) was 11%.

Phenolic and Flavonoid Content of the Extract. Phenols and flavonoids belong to a large family of secondary metabolites produced by plants that have multiple roles in plant metabolism primarily in plant defense.²⁸ As a result of their multifunctional capabilities of hydrogen donating, reducing, and singlet oxygen quenching, these phenols and flavonoids can neutralize free radicals. The total phenolic value in MHPM was 15.7 %.

Flavonoids are a class of naturally occurring phenylchromones that can be found in various parts of plant materials. Total flavonoid content in MHPM was 7.8 %. A previous study also reported that *Pterocarpus marsupium* contains a high concentration of phenolic and flavonoids.²⁹ On the basis of their phenolic and flavonoid content, MHPM may be a good source of bioactive compounds.

Antioxidant Potential of MHPM. In the DPPH assay, the degree of discoloration indicates the scavenging potency of antioxidant metabolites. Secondary metabolites found in MHPM including phenols, flavonoids, and terpenoids may be involved in the elevation of antioxidant potential due to their redox properties.^{28,30} A previous study also reported that *Pterocarpus marsupium* contains a high concentration of phenolic and flavonoids.²⁹ The free radical scavenging potency of MHPM showed dose-dependent scavenging potential, and the scavenging potency at 500 μ g/mL was $68.58 \pm 3.471\%$, with an IC_{50} value of 156.342 ± 10.70 μ g/mL. The positive control (ascorbic acid) exhibited an average inhibition of $79.69 \pm 3.35\%$ at the concentration of 500 μ g/mL with an IC_{50} value of 50.03 ± 5.29 μ g/mL. MHPM manifested a statically significant *P*-value summary*** and *P*-value (one-tailed) < 0.0001 redox potential

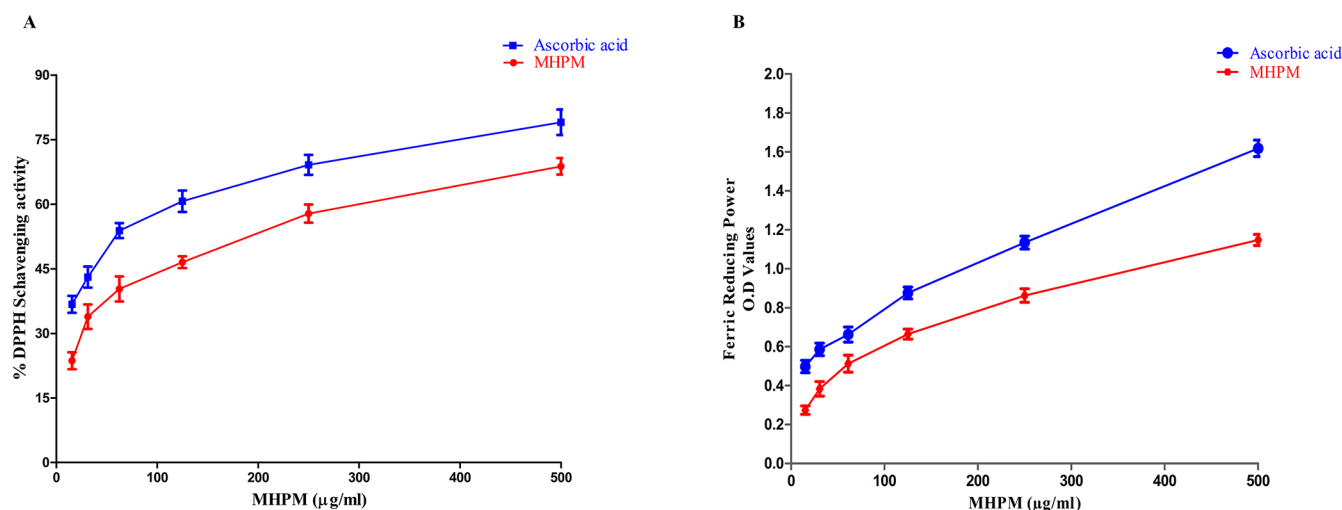


Figure 1. Free radical scavenging (A) and reducing power (B) capacity of MHPM.

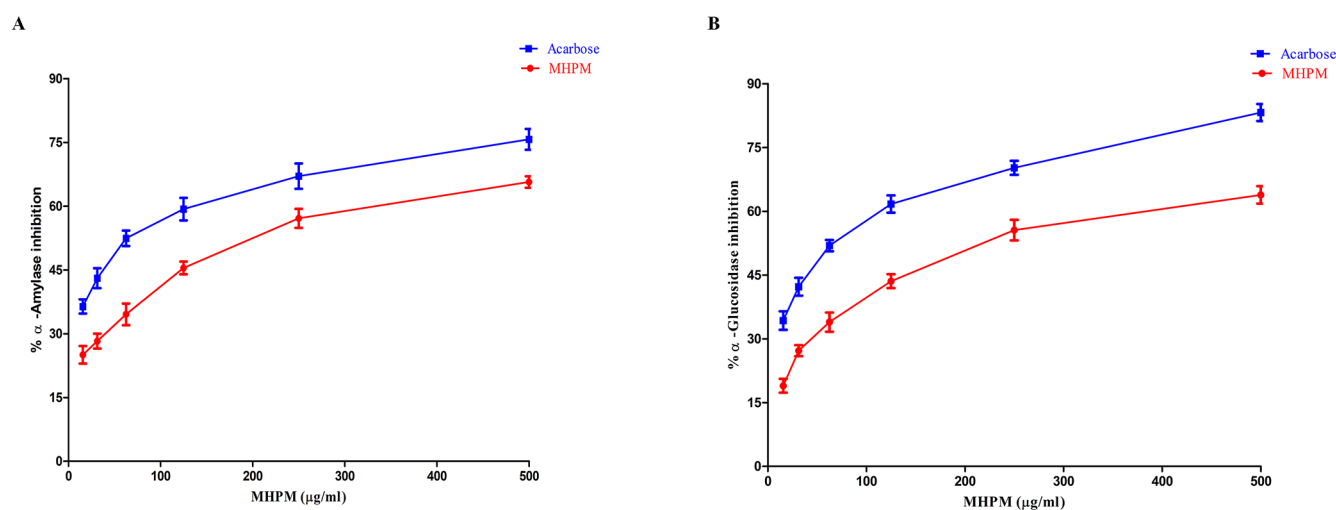


Figure 2. α -Amylase (A) and α -glucosidase (B) inhibitor activity of MHPM.

when compared to ascorbic acid. The reducing power of the MHPM from ferricyanide into ferrocyanide was conducted to confirm its antioxidant potential. The increase in antioxidant activity was observed and was linearly proportionate to the DPPH scavenging activity (Figure 1).

The antioxidant activity of MHPM could be attributed to the presence of phenols and flavonoids. A higher phenolic and flavonoid content coincides with high antioxidant activity.³¹ One of the studies reported that the leaf extract of *Pterocarpus marsupium* showed high antioxidant activity and may be due to the high content of polyphenols.³² These polyphenols complement the efficacy of the antioxidant enzyme defense system, containing a variety of enzymes, including superoxide dismutase, glutathione peroxidase, glutathione reductase, and catalase. These enzymes are well-known for their crucial role in the suppression of excessive ROS by breaking the autoxidation chain of events, sniffing out trace elements, and attempting to prevent overall cell damage. The antioxidant activities of medicinal herbs and nutritional supplements are dependent on a large cohort of polyphenols, which are naturally occurring antioxidants that play an important role in oxidative suppression and cure various ailments including T2DM.³³

Enzyme Inhibitory Activity. α -Amylase Inhibitory Potential of MHPM. The metalloenzyme α -amylase is a calcium-containing key enzyme that breaks down polysaccharide-1,4 linkages to monosaccharides in the oral cavity. An increase in postprandial blood sugar levels can be caused by an uneven cellular carbohydrate and lipid metabolism, which inevitably leads to the initiation and advancement of T2DM. As a result, finding alternative therapies that inhibit α -amylase is critical. MHPM exhibited strong dose-dependent α -amylase inhibitory activity with an average inhibition of $66.441 \pm 3.459\%$, at $500 \mu\text{g/mL}$ and an IC_{50} value of $158.663 \pm 10.986 \mu\text{g/mL}$. The percentage inhibition of positive control (acarbose) was $78.410 \pm 4.005\%$ at $500 \mu\text{g/mL}$, with an IC_{50} value of $56.060 \pm 4.465 \mu\text{g/mL}$. MHPM showed statically significant P -value summary*** and P -value (one-tailed) < 0.0001 α -amylase inhibitory potential when compared to acarbose. As a result, the study suggests that the MHPM has a good ability to inhibit α -amylase as shown in Figure 2A.

α -Amylase inhibitors prevent or slow the uptake of starch into the gastrointestinal tract (GIT), primarily by inhibiting the hydrolysis of 1,4-glycosidic linkages in starch and other oligosaccharides into maltose and other simple sugars.³⁴ Several

studies show that amylase blockers, notably acarbose (pseudotetrascaccharide), can regulate the modulatory effects of PPG and HbA1c in high blood sugar.³⁵ Ineffective treatment promotes slow progression of T2DM and leads to oxidative stress because of the generation of free radicals as a result of glucose oxidation and the oxidative degradation of glycosylated proteins in diabetic patients leading to the complication of the disease. Therefore, natural products rich in polyphenols can help in alleviating diabetic complications.³⁶

α -Glucosidase Inhibitory Potential of MHPM. In type 2 diabetes patients, the α -glucosidase enzyme can significantly raise postprandial blood glucose levels. As a result, α -glucosidase inhibitors control postprandial hyperglycemia by postponing carbohydrate metabolism.³⁷ PM is one of the most credible natural and alternative therapies with many pharmacological properties including an inhibitory potential against the α -glucosidase activity.³⁸ The findings indicated a significant dose-dependent inhibition activity with a mean inhibitory percentage of $63.852 \pm 3.535\%$ at $500 \mu\text{g/mL}$, with an IC_{50} value of $180.21 \pm 11.35 \mu\text{g/mL}$, whereas acarbose showed a mean inhibitory percentage of $82.901 \pm 4.019\%$ at $500 \mu\text{g/mL}$ with an IC_{50} value of $57.969 \pm 6.835 \mu\text{g/mL}$. MHPM showed statically significant P -value summary*** and P -value (one-tailed) < 0.0001 α -glucosidase inhibitory potential when compared to acarbose. As a result, the study reveals that MHPM α -glucosidase inhibitory potential increases with the increase in concentration and further remains constant at higher concentrations as shown in Figure 2B. The ability to inhibit enzymes may be credited to the high phenolic and flavonoid content of MHPM. The presence of essential phytoconstituents, viz., quercetin, epicatechin, and vanillic acid, may contribute to the enzyme inhibition capacity of MHPM.^{39,40}

TLC Fingerprint Profile of MHPM. Thin-layer chromatography was used to separate the metabolites of MHPM. For better separation of metabolites in MHPM, different mobile phases with different ratios were examined. The mobile phase toluene/ethyl acetate/methanol/formic acid [6:3:0.5:0.5] showed well-defined peaks with satisfying resolution at different Rf values. The TLC fingerprinting for MHPM resolved the existence of 16 peaks corresponding to different metabolites at each peak. A total 16 peaks with retention factor (Rf) values of 0.05, 0.14, 0.20, 0.23, 0.29, 0.40, 0.44, 0.47, 0.50, 0.56, 0.67, 0.74, 0.79, 0.85, 0.89, and 0.94, respectively, at 254 nm and 12 peaks correspond to different metabolites at each peak with (Rf) values of 0.14, 0.20, 0.23, 0.29, 0.37, 0.40, 0.44, 0.47, 0.67, 0.75, and 0.85 are separated and visualized at 366 nm (Table 1). The analysis of quality control for herbal-based medicines is one of the critical problems. TLC profiling is a typical tool for separating metabolite patterns from natural products. Plant materials or extracts with the same TLC pattern must have the same bioactivity. Quality control and regulatory bodies can use TLC profiling of plant materials to verify product quality and safety.

TLC-MS Bioautographic Activity. Identified Free Radical Scavenging Metabolite by TLC-MS-Bioautography. Mass spectrometry has become a technique of choice for identifying the quantity and chemical diversity of plant metabolites. Low resolution mass spectroscopy is preferred for the identification and quantification of low-abundance metabolites, without their fragmentation because of its minimal analysis cost, robustness, and great efficiency.^{23,41} TLC interfaced with mass spectrometry is a fast and effective method for direct identification of bioactive compounds present in the plant extract having antioxidant or enzyme inhibitory activities.^{21,42,43} To identify a DPPH

Table 1. Phytochemicals Identified in MHPM by HPTLC Analysis

S. no.	Rf value	area in AU		identified compounds by TLC-MS-bioautography
		254 nm	366 nm	
01	0.05	+	–	–
02	0.14 ^a	+	+	epicatechin
04	0.20	+	+	–
06	0.23	+	+	–
07	0.29	+	+	–
08	0.37	–	+	–
09	0.40 ^a	+	+	quercetin
10	0.44 ^a	+	+	naringenin
11	0.47	+	+	–
12	0.50	+	–	–
13	0.56	+	–	–
14	0.67 ^{a,b}	+	+	vanillic acid
15	0.74	+	–	–
16	0.75	–	+	–
17	0.79	+	–	–
18	0.85	+	+	–
19	0.89	+	–	–
20	0.94	+	–	–

^aAntioxidant. ^bAntidiabetic.

scavenging metabolite by TLC-bioautography hyphenated with mass spectroscopy, the previously developed TLC plate was dipped in DPPH solution and examined under visible light; the presence of pale-yellow bands on a purple background confirmed the free radical scavenging metabolites. Four metabolites, viz., epicatechin (Rf 0.14), quercetin (Rf 0.40), Naringenin (Rf 0.44), and vanillic acid (Rf 0.67), have been identified through MS analysis of scrapped bands as shown in Figure 3 and as mentioned in Table 2. These metabolites have been previously reported in the heartwood of PM⁴⁴ and are reported to be having strong free radical scavenging activity;⁴⁵ moreover, vanillic acid had been reported to show both antioxidant and antihyperglycemic potential.⁴⁶

Many authors propose that active molecules from natural herbs act antagonistically to various diseases such as diabetes.⁴⁷ Oxidative stress causes a variety of pathophysiological events, leading to diabetic complications; the antioxidant activity of bioactive compounds may neutralize the free radicals and thus may account for their potential health benefits in ROS induced metabolic disorders. The results showed the promising antioxidant potential of MHPM through TLC-bioautography evidenced by its metabolites composition.

Identified α -Amylase Inhibitor Metabolite by TLC-MS-Bioautography. The TLC plate with α -amylase inhibitor activity was visualized under visible light, and a dark colored alpha-amylase inhibitory band on the light violet background was observed. Furthermore, the MS analysis of the scrapped active band from the TLC plate indicated one prominent bioactive compound as vanillic acid (Rf 0.67), as shown in Figure 3 and mentioned in Table 2.

Vanillic acid has been reported to show a strong inhibitory effect on α -amylase by Alexandre et al.⁴⁸ Vanillic acid was also reported to have a modulatory influence on diabetic hypertension control, lowering blood glucose and blood pressure while also countering oxidative stress through tissue antioxidant activation.⁴⁹ In this study, vanillic acid (Rf 0.67) showed both DPPH inhibition and α -amylase inhibitory activity, and this

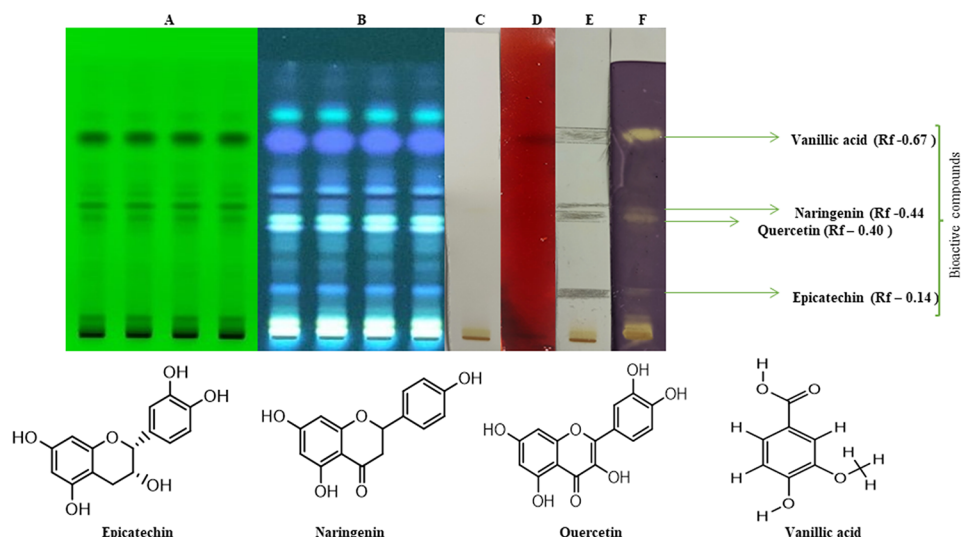


Figure 3. The photograph of the developed TLC plate of MHPM at 254 and 366 nm (3A and 3B); TLC-bioautography representing the normal view (control TLC) of the plate (3C); α -amylase-treated TLC bioautogram of MHPM, displaying dark blue/violet spots on a brown color background (3D); scrapped α -amylase active spot and DPPH active spots from TLC plates (3E) and DPPH scavenged treated TLC bioautogram of MHPM displaying yellow spots against a dark purple background (3F).

Table 2. Identified Active Compounds from MHPM through TLC-Bioautography-MS

TLC Rf value	compound identified	exact mass	tentative mass ^a	mass error [Da]	molecular formula	mass ID	activities
0.14	epicatechin	290.0790	289.0021	-0.0769	C ₁₅ H ₁₄ O ₆	MBID: 000088	antioxidant
0.40	quercetin	302.0422	301.0305	-0.0117	C ₁₅ H ₁₀ O ₇	MBID: PN000111	antioxidant
0.44	naringenin	272.0685	273.0069	-0.0616	C ₁₅ H ₁₂ O ₅	MBID: ML005001	antioxidant
0.67	vanillic acid	168.1467	167.9883	0.8416	C ₈ H ₈ O ₄	NIST ID: 121-34-6	antioxidant and amylase activity

^aObserved mass [M - H] or [M + H].

inhibitory effect of vanillic acid makes it a strong candidate drug against diabetes; however, further studies are needed to isolate the inhibitory compound from MHPM and establish the findings using a suitable molecular approach.

Identified Metabolites in MHPM through UPLC-MS. UPLC-MS analysis was performed to identify the various metabolites present in MHPM. UPLC-MS is the most acceptable method for identifying tangible and intangible metabolites.³³ The tentative mass observed was matched with the mass records from authentic sources using a mass bank, a chemical library, and a literature survey. UPLC-MS analysis indicates the presence of 40 phytoconstituents in MHPM as mentioned in Table 3. The prominent antidiabetic compounds identified in MHPM are pterostilbene (R_t 5.289),⁵⁰ epicatechin (R_t 1.722),⁵¹ curcumol (R_t 4.735),⁵² amygdalin (R_t 12.256),⁵³ quercetin (R_t 4.735),⁵⁴ iso-liquiritigenin (R_t 5.289),⁵⁵ naringenin (R_t 0.615),⁵⁶ kaempferol-7-O- α -L-rhamnoside (R_t 4.735),⁵⁷ lupeol (R_t 9.010),⁵⁸ and epigallocatechin gallate (R_t 8.703).⁵⁹

We reported the tentatively identified phytoconstituents including some major antidiabetic compounds from the heartwood extract of PM. For epicatechin (R_t 1.722), a natural flavonoid, several studies of its isolation from the bark of PM reported that it alleviated hyperglycemia and showed free radical scavenging activity.^{60,61} Pterostilbene (R_t 5.289) is a stilbenoid structurally similar to resveratrol and is one of the main constituents of PM; pterostilbene is reported to be antidiabetic and alleviate diabetes in streptozotocin-induced diabetic mice.⁶² Iso-liquiritigenin (R_t 5.289) is a phenolic phytoconstituent, is a part of the class of chalcones, exhibited antioxidant and

antidiabetic properties, and has previously been isolated from the heartwood of *Pterocarpus santalinus*.⁶³ Various other glycosyloxyflavones and alkaloids have been identified in MHPM that may be responsible for their antioxidant and antidiabetic activity.

In Silico Analysis of PTP1B Inhibitors. Virtual Screening Based on Molecular Docking. Virtual screening is a method of identifying potential compounds by comparing them to predetermined biological targets.⁶⁴ It has become a necessary technique in terms of reducing experimental time and energy. Virtual screening using molecular docking was carried out with protein tyrosine phosphatase (PTP-1B), which has recently been introduced to be a negative regulator of the signaling pathway, proposing that inhibition of this enzyme could help with type 2 diabetes treatment.⁶⁵ We initially select the 10 best antidiabetic compounds from MHPM out of which six phytoconstituents showed good docking scores, viz., epicatechin, quercetin, pterostilbene, vanillic acid, naringenin, and amygdalin, based on their significantly low binding energies with PTP-1B (Table 4). Here, we found that the epicatechin showed good binding affinity followed by quercetin and cocrystal with PTP-1B and preferentially occupied the active site cavity with high ligand efficacy with the binding free energy of -8.2 kcal/mol with PTP-1B; when compared with the cocrystal, both the compounds formed several close interactions, such as hydrogen bonds, to active site residues and other interactions offered by the protein PTP-1B as shown in Table 4, lower panel. We used PyMOL and Discovery Studio Visualizer to conduct a complete analysis of epicatechin and quercetin for their specific

Table 3. List of Phytoconstituents Identified by UP-LCMS in MHPM

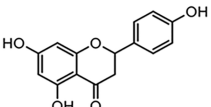
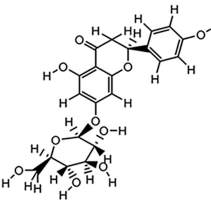
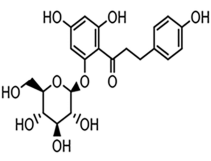
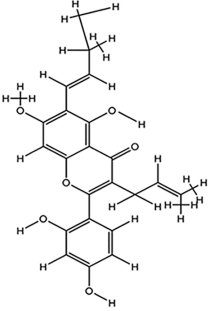
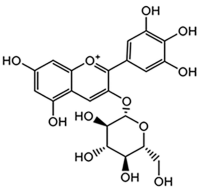
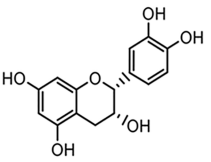
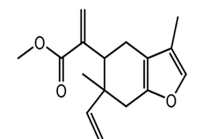
RT	Tentative Mass ^a	Exact Mass	Mass Error [Da]	Phytoconstituent	Formula	Structure	Mode	Mass bank record.
0.615	271.1869	272.0685	0.1184	Naringenin	C ₁₅ H ₁₂ O ₅		Negative	MBID:M L005001
	433.0105	434.1213	-0.1108	Naringenin-7-O-glucoside	C ₂₁ H ₂₂ O ₁₀		Negative	MBID: BS003367
	435.0909	436.1369	-0.0460	Phloridzin	C ₂₁ H ₂₄ O ₁₀		Negative	MBID: CE000071
	435.0909	436.1886	-0.0977	Artocaprin	C ₂₆ H ₂₈ O ₆		Negative	MBID: MBID: BS003597
	464.8660	465.1033	0.1627	Delphinidin-3-O-beta-glucopyranoside	C ₂₁ H ₂₁ O ₁₂		Negative	MBID: PR10091 2
1.722	289.0672	290.0790	-0.0118	Epicatechin	C ₁₅ H ₁₄ O ₆		Negative	MBID: 000088
2.429	259.1586	260.1412	0.0174	Isoserinenine	C ₁₆ H ₂₀ O ₃		Negative	MBID: JP003659

Table 3. continued

RT	Tentative Mass ^a	Exact Mass	Mass Error [Da]	Phytoconstituent	Formula	Structure	Mode	Mass bank record.
4.735	301.0952	302.0422	0.0530	Quercetin	C ₁₅ H ₁₀ O ₇		Negative	MBID: PN000111
	235.7505	236.1776	0.5729	Curcumol	C ₁₅ H ₂₄ O ₂		Negative	MBID: FIO01064
	430.8651	432.1056	-0.2405	Kaempferol-7-O-alpha-L-rhamnoside	C ₂₁ H ₂₀ O ₁₀		Negative	MBID: PR100942
	469.3517	470.1940	0.1577	Limonin	C ₂₆ H ₃₀ O ₈		Negative	MBID: TY000204
5.289	255.0618	256.2569	-0.1951	Isoliquiritigenin	C ₁₅ H ₁₂ O ₄		Negative	MBID: PR302707
		256.3009	-0.2391	Pterostilbene	C ₁₆ H ₁₆ O ₃		Negative	MBID: PR304273
		256.0735	-0.0117	Pinocembrin	C ₁₅ H ₁₂ O ₄		Negative	MBID: BML00869
7.872	236.1406	237.0789	0.0617	1-Amino-2-methylantraquinone	C ₁₅ H ₁₁ NO ₂		Negative	MBID: LU077301

Table 3. continued

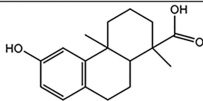
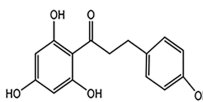
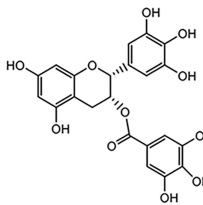
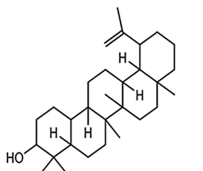
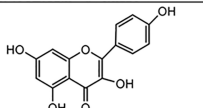
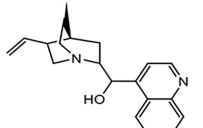
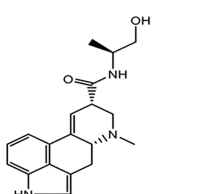
RT	Tentative Mass ^a	Exact Mass	Mass Error [Da]	Phytoconstituent	Formula	Structure	Mode	Mass bank record.
8.703	273.8527	274.1568	0.6959	Podocarpic acid	C ₁₇ H ₂₂ O ₃		Negative	MBID: BML8198 8
		274.0841	0.7686	Phloretin	C ₁₅ H ₁₄ O ₅		Negative	MBID: BML8193 3
	458.0399	458.0849	0.9550	Epigallocatechin gallate	C ₂₂ H ₁₈ O ₁₁		Negative	MBID: TY000083
9.010	426.8343	426.3861	1.44782	Lupeol	C ₃₀ H ₅₀ O		Negative	Pubchem CID:2598 46
9.994	285.8163	286.0477	0.7686	Kaempferol	C ₁₅ H ₁₀ O ₆		Negative	MBID: TY000225
14.14 6	293.0333	294.1730	-0.1397	Cinchonine	C ₁₉ H ₂₂ N ₂ O		Negative	MBID: BML8004 0
	324.9569	325.1790	0.7779	Ergometrinine	C ₁₉ H ₂₃ N ₃ O ₂		Negative	MBID: AC00031 8

Table 3. continued

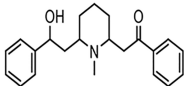
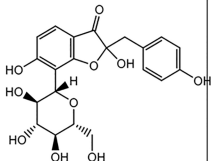
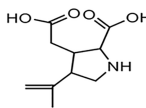
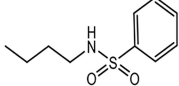
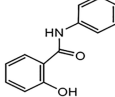
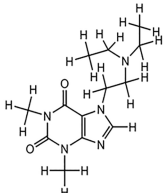
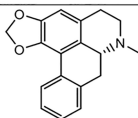
RT	Tentative Mass ^a	Exact Mass	Mass Error [Da]	Phytoconstituent	Formula	Structure	Mode	Mass bank record.
0.63s	338.2853	337.20419	0.08111	Lobeline	C ₂₂ H ₂₇ NO ₂		Positive	MBID: BML8162 2
	434.8958	434.1212	-0.2254	Marsuposide	C ₂₁ H ₂₂ O ₁₀		Positive	Pubchem CID: 9932617
	214.0980	213.2330	-0.1350	Kainic acid	C ₁₀ H ₁₅ NO ₄		Positive	MBID: PR304850
	213.08235	0.01565	N-Butylbenzenesulfonamide	C ₁₀ H ₁₅ NO ₂ S		Positive	MBID: AU22995 7	
	213.07899	0.01901	Salicylanilide	C ₁₃ H ₁₁ NO ₂		Positive	MBID: LU115551	
1.737	280.4847	279.1695	0.3152	Etamiphylline	C ₁₃ H ₂₁ N ₅ O ₂		Positive	MBID: CO00018 1
	279.3417	0.1430	Roemerine	C ₁₈ H ₁₇ NO ₂		Positive	MBID: NGA0089 4	

Table 3. continued

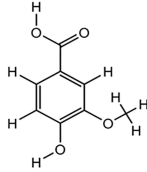
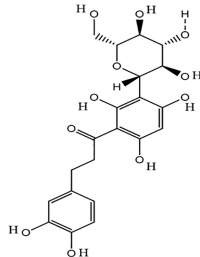
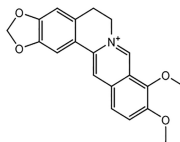
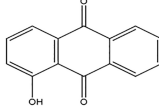
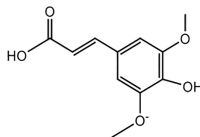
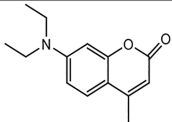
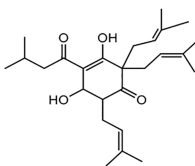
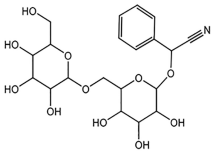
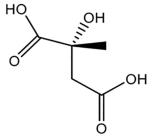
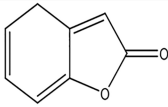
RT	Tentative Mass ^a	Exact Mass	Mass Error [Da]	Phytoconstituent	Formula	Structure	Mode	Mass bank record.
2.937	169.9460	168.1467	0.7993	Vanillic acid	C ₈ H ₈ O ₄		Positive	NIST ID:121- 34-6
	453.4240	452.1319	0.2921	Aspalathin	C ₂₁ H ₂₄ O ₁₁		Positive	MBID: BS003543
3.890	336.9200	336.1235	-0.2035	Berberine	[C ₂₀ H ₁₈ NO] +		Positive	MBID: KO00888 6
4.720	225.1519	224.04730	0.1046	1-Hydroxyanthraquinone	C ₁₄ H ₈ O ₃		Positive	MBID: UA00250 1
6.012	225.1519	224.0684	0.0835	Sinapic acid	C ₁₁ H ₁₂ O ₅		Positive	MBID: PR020014

Table 3. continued

RT	Tentative Mass ^a	Exact Mass	Mass Error [Da]	Phytoconstituent	Formula	Structure	Mode	Mass bank record.
6.473	232.8245	231.1259	0.6986	7-Diethylamino-4-methylcoumarin	C ₁₄ H ₁₇ NO ₂		Positive	MBID: LU043201
	415.3272	414.2770	0.0502	Lupulone	C ₂₆ H ₃₈ O ₄		Positive	MBID: BS003134
	458.1699	457.15842	0.0115	Amygdalin	C ₂₀ H ₂₇ NO ₁₁		Positive	MBID: TY000092
12.254	149.2672	148.0371	0.2301	Citramalic acid	C ₅ H ₈ O ₅		Positive	MBID: PR100302
13.884	134.1806	134.0367	-0.8561	2(4H)-Benzofuranone	C ₈ H ₆ O ₂		Positive	Pubchem CID: 57430039

^aObserved mass [M – H] or [M + H].

Table 4. Binding Affinity of Compounds with PTP1B Generated from Molecular Docking (Upper Panel) and Molecular Interaction of Epicatechin and Quercetin with PTP1B Binding Site along with the Key Interacting Residues (Lower Panel)

target protein	name of the ligand	binding free energy (kcal/mol)	PKi	ligand efficiency (kcal/mol/non-H atom)
protein tyrosine phosphatase 1B (PTP1B) (PDB ID: 1C83)	epicatechin	-8.2	4.91	0.224
	quercetin	-7.7	4.89	0.223
	pterostilbene	-6.7	4.87	0.218
	vanillic acid	-6.7	4.84	0.213
	naringenin	-6.6	4.80	0.174
	amygdalin	-6.5	4.71	0.170
	co-crystal	-8.3	4.91	0.319
	protein–ligand interactions			
hydrogen bonds				
compound	affinity (kcal/mol)	amino acid residues	distance (Å)	other interacting residues
epicatechin	-8.2	Thr-133	2.35	-
		Asn-134	2.38	
		Thr-158	2.43	
		Gln-59	2.68	
quercetin	-7.7	Gln-127	2.98	Arg-156,Ile-149,Thr-151
		Glc-147	2.59	
		Lys-150	2.46, 2.72	

interactions with the PTP1B binding sites. The molecular docking study provides an accurate and preferred orientation of a compound at the binding site of a receptor. For proper function, the PTP1B binding site at the main catalytic center of

PTP1B is critical. According to the docking analysis, epicatechin and quercetin bind in the same site as the cocrystallized ligand. As a result, it is clear that epicatechin and quercetin could act as PTP1B inhibitors. Interaction analysis of all possible docked

Table 5. Parameters Calculated for Protein and Protein–Ligand Systems after 100 ns Simulation

	MD simulation parameters								
	average RMSD (nm)	average RMSF (nm)	average Rg (nm)	average SASA (nm ²)	kinetic energy (kJ/mol)	potential energy (kJ/mol)	enthalpy (kJ/mol)	volume (nm ³)	density (kg/m ³)
tyrosine phosphatase 1b	0.351137	0.1494	1.89354	134.992	160029	−973265	−813198	637.851	1025.4
tyrosine phosphatase 1b-epicatechin complex	0.355333	0.1809	1.90585	139.833	112422	−601159	−488709	459.992	1008.44

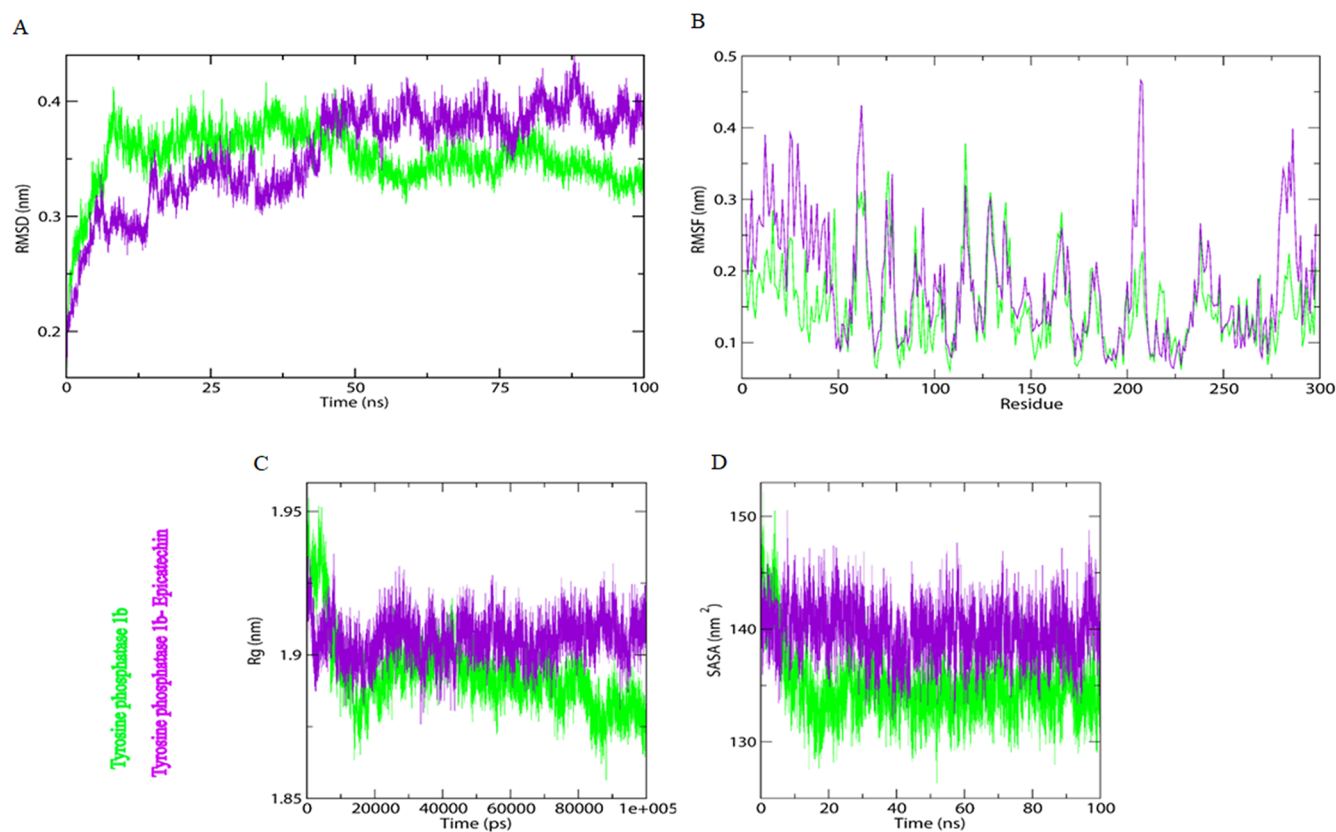


Figure 6. (a) Root mean square deviation (RMSD) for epicatechin in complex with PTP1B Mpro. (b) Root mean square fluctuations (RMSF) for epicatechin in complex with PTP1B Mpro. (c) Time evolution of the radius of gyration (Rg) for epicatechin in complex with PTP1B Mpro. (d) Solvent accessible surface area (SASA) for epicatechin in complex with PTP1B Mpro.

representing the PTP1B inhibitory effect by the identified compounds is shown in Figure 5.

Molecular Dynamics (MD) Simulation Studies of PTP-1B and Epicatechin to Combat Insulin Resistance. MD simulations can help in understanding the structural details and dynamic behavior of protein–ligand complexes where experimental approaches struggle to provide specific insight. MD simulation results of PTP-1B alone and in combination with epicatechin were carried out with a GROMOS 96 force field in GROMACS 5.1.2. To determine conformational dynamics, the bioactive constituent “epicatechin” was chosen for MD simulations based on its binding energy and significant interactions with the target molecule. As a result, PTP-1B and epicatechin were prepared and used for 100 ns MD simulation. The stability and dynamics of PTP-1B in complex with the ligands epicatechin as well as the apo-state of PTP-1B were studied using a variety of comprehensive and structural parameters. Following that, all-atom MD simulations (100 ns) of PTP-1B alone and in complex with epicatechin were run to determine conformational dynamics in an aqueous environment. Several parameters, including root-mean-square deviation

(RMSD), studying root-mean-square fluctuation (RMSF), the radius of gyration (Rg), and solvent accessible surface area (SASA), as well as the systems’ kinetic energy, enthalpy, potential energy, and density, were calculated and presented in Table 5. It is well understood that the linkage of any ligand causes conformational changes in the target protein’s native structure. The degree of these conformational changes with time from the data produced by the MD simulation is measured by evaluating the RMSD.⁶⁶ RMSD plots of the PTP-1B apo and PTP-1B-epicatechin complex are presented in Figure 6. Average RMSD values for PTP-1B apo and the PTP-1B-epicatechin complex were found to be 0.351137 and 0.355333 nm, respectively, as mentioned in Table 5. RMSD shows that the binding of the epicatechin with PTP-1B were balanced throughout the simulation, suggesting substantial stability of the docked system. The Rg values provide information about the protein’s overall dimensions and shape.⁶⁶ The Rg values for the PTP-1B apo and the PTP-1B-epicatechin complex were discovered to be 1.89354 and 1.90585 nm, respectively. These Rg values indicate that the protein’s overall shape was stable after epicatechin binding. Electrostatic and surface properties were

further studied, and SASA calculations provide insight into the interaction between a protein and its bordering solvent, reflecting their conformational behavior patterns during simulation.⁶⁷ In the complex, a small increase in SASA was observed, which could be due to the higher surface area of PTP-1B in the involvement of epicatechin, exposing some inner residues to the exterior. Throughout the simulation, the SASA maintained a stable equilibrium without switching, indicating structural stability of PTP-1B in the presence of epicatechin. The energy released during the bonding process establishment or, so, the engagement of a ligand with another ligand and protein is represented by binding energy.⁶⁸ Lower binding energy indicates better ligand–protein binding. The results show that all types of energy played a positive role in the interaction between PTP-1B and epicatechin.

PTP-1B is the main enzyme involved in insulin receptor desensitization and can be a drug target for the treatment of diabetes type 2. PTP-1B inhibitors have already been discovered that interact with the enzyme's binding site, which is located around the catalytic amino acid Cys215 and the surrounding area.⁶⁹ The current study shows that the phytoconstituent “epicatechin” is efficacious with potent inhibition against PTP-1B. We further suggest that this small inhibitor biochemical constituent should be validated and repurposed for the treatment of T2DM. Binding studies of this inhibitor molecule with a purified target protein are needed to confirm the preliminary findings.

CONCLUSION

MHPM showed the presence of vital bioactive compounds which may show a variety of biochemical functions. The TLC-bioautographic analysis combined with MS analysis revealed that MHPM has antidiabetic and antioxidant compounds. The results indicate that MHPM has an enormous ability to be used as a therapeutic agent against diabetes and oxidative stress, mitigated by α -amylase and α -glucosidase, rescuing oxidative stress by free-radical scavenging. The enzyme inhibitory potential could help to lower postprandial blood sugar levels. The bioactive constituent epicatechin was discovered to be a potent inhibitor of PTP-1B in this study. Binding studies and bioassays using epicatechin as an inhibitor against purified PTP-1B protein are needed to confirm these findings further using suitable *in vitro* and/or *in vivo* models.

AUTHOR INFORMATION

Corresponding Author

Sayeed Ahmad – Centre of Excellence in Unani Medicine (Pharmacognosy & Pharmacology) and Bioactive Natural Product Laboratory, School of Pharmaceutical Education and Research, Jamia Hamdard, New Delhi 110062, India; orcid.org/0000-0003-1573-152X; Phone: 91-9891374647; Email: sahmad_jh@yahoo.co.in; Fax: 00-91-11-26059663

Authors

Mohammad Irfan Dar – Department of Biotechnology, Jamia Millia Islamia, New Delhi 110025, India

Mohammad Irfan Qureshi – Department of Biotechnology, Jamia Millia Islamia, New Delhi 110025, India

Sultan Zahiruddin – Centre of Excellence in Unani Medicine (Pharmacognosy & Pharmacology) and Bioactive Natural Product Laboratory, School of Pharmaceutical Education and Research, Jamia Hamdard, New Delhi 110062, India

Sageer Abass – Department of Biotechnology, Jamia Millia Islamia, New Delhi 110025, India

Bisma Jan – Centre of Excellence in Unani Medicine (Pharmacognosy & Pharmacology) and Bioactive Natural Product Laboratory, School of Pharmaceutical Education and Research, Jamia Hamdard, New Delhi 110062, India; Department of Food Technology School of Interdisciplinary Science & Technology, Jamia Hamdard, New Delhi 110062, India

Armiya Sultan – Department of Biotechnology, Jamia Millia Islamia, New Delhi 110025, India

Complete contact information is available at:

<https://pubs.acs.org/10.1021/acsomega.2c04283>

Notes

The authors declare no competing financial interest.

ACKNOWLEDGMENTS

Authors would like to acknowledge the Indian Council of Medical Research (ICMR), New Delhi, India, for providing a scholarship to Mohammad Irfan Dar (45/10/2022/TRM/BMS) to carry out the present research work.

REFERENCES

- (1) Sun, X.; Yu, W.; Hu, C. Genetics of Type 2 Diabetes: Insights into the Pathogenesis and Its Clinical Application. *BioMed. Research International*. **2014**, 926713.
- (2) Patergnani, S.; Bouhamida, E.; Leo, S.; Pinton, P.; Rimessi, A. Mitochondrial Oxidative Stress and “mito-Inflammation”: Actors in the Diseases. *Biomedicines*. **2021**, 9 (2), 216.
- (3) Saisho, Y. Importance of Beta Cell Function for the Treatment of Type 2 Diabetes. *J. Clin Med*. **2014**, 3 (3), 923–943.
- (4) King, H.; Aubert, R. E.; Herman, W. H. Global Burden of Diabetes, 1995–2025: Prevalence, Numerical Estimates, and Projections. *Diabetes Care* **1998**, 21 (9), 1414–31.
- (5) Lipinski, B. Pathophysiology of Oxidative Stress in Diabetes Mellitus. *J. Diabetes Complications* **2001**, 15, 203–10.
- (6) Marín-Peñalver, J. J.; Martín-Timón, I.; Sevillano-Collantes, C.; Cañizo-Gómez, F. J. d. Update on the Treatment of Type 2 Diabetes Mellitus. *World J. Diabetes* **2016**, 7, 354–395.
- (7) Chang, H. Y.; Wallis, M.; Tiralongo, E. Use of Complementary and Alternative Medicine among People Living with Diabetes: Literature Review. *J. Adv. Nurs* **2007**, 58, 307–319.
- (8) Dey, L.; Attele, A. S.; Yuan, C. S. Alternative Therapies for Type 2 Diabetes. *Alternative Medicine Review*. **2002**, 7 (1), 45–58.
- (9) Verma, S.; Gupta, M.; Popli, H.; Aggarwal, G. Diabetes Mellitus Treatment Using Herbal Drugs. *Int. J. Phytomedicine* **2018**, 10 (1), 01.
- (10) Therrell, M. D.; Stahle, D. W.; Mukelabai, M. M.; Shugart, H. H. Age, and Radial Growth Dynamics of *Pterocarpus Angolensis* in Southern Africa. *For Ecol Manage* **2007**, 244, 24–31.
- (11) Vijayan, D.; G, S. *Pterocarpus Marsupium* for the Treatment of Diabetes and Other Disorders. *J. Complement Med. Altern Healthc* **2019**, DOI: 10.19080/jcmah.2019.09.555754.
- (12) Perera, H. Antidiabetic Effects of *Pterocarpus Marsupium* (Gammalu). *European J. Med. Plants* **2016**, 13, 1–14.
- (13) Ministry for Health and Family Welfare. *The Ayurvedic Pharmacopoeia of India*; 2010; Vol. 1, p 11.
- (14) Khan, W.; Parveen, R.; Chester, K.; Parveen, S.; Ahmad, S. Hypoglycemic Potential of Aqueous Extract of Moringa Oleifera Leaf and in Vivo GC-MS Metabolomics. *Front Pharmacol* **2017**, 8, 577.
- (15) Saeed, N.; Khan, M. R.; Shabbir, M. Antioxidant Activity, Total Phenolic and Total Flavonoid Contents of Whole Plant Extracts *Torilis Leptophylla* L. *BMC Complement Altern Med*. **2012**, 12, 221.
- (16) Liu, S. C.; Lin, J. T.; Wang, C. K.; Chen, H. Y.; Yang, D. J. Antioxidant Properties of Various Solvent Extracts from Lychee (*Litchi Chinensis* Sonn.) Flowers. *Food Chem*. **2009**, 114, 577–581.

- (17) Zahiruddin, S.; Khan, W.; Nehra, R.; Alam, M. J.; Mallick, M. N.; Parveen, R.; Ahmad, S. Pharmacokinetics and Comparative Metabolic Profiling of Iridoid Enriched Fraction of Picrorhiza Kurroa - An Ayurvedic Herb. *J. Ethnopharmacol* **2017**, *197*, 157–164.
- (18) Ademiluyi, A. O.; Oboh, G. Soybean Phenolic-Rich Extracts Inhibit Key-Enzymes Linked to Type 2 Diabetes (α -Amylase and α -Glucosidase) and Hypertension (Angiotensin I Converting Enzyme) in Vitro. *Exp Toxicol Pathol* **2013**, *65* (3), 305–9.
- (19) Shai, L. J.; Magano, S. R.; Lebelo, S. L.; Mogale, A. M. Inhibitory Effects of Five Medicinal Plants on Rat Alpha-Glucosidase: Comparison with Their Effects on Yeast Alpha-Glucosidase. *J. Med. Plants Res.* **2011**, *5* (13), 2863–2867.
- (20) Rab, R. A.; Zahiruddin, S.; Ibrahim, M.; Husain, F.; Parveen, R.; Khan, W.; Ahmad, F. J.; Khan, A. A.; Ahmad, S. HPTLC and UPLC-MS/MS Methods for Quality Control Analysis of Itrifal Formulations of Unani System of Medicine. *J. AOAC Int.* **2020**, *103*, 649–658.
- (21) Gaurav; Zahiruddin, S.; Parveen, B.; Ibrahim, M.; Sharma, I.; Sharma, S.; Sharma, A. K.; Parveen, R.; Ahmad, S. TLC-MS Bioautography-Based Identification of Free-Radical Scavenging, α -Amylase, and α -glucosidase Inhibitor Compounds of Antidiabetic Tablet BGR-34. *ACS Omega* **2020**, *5* (46), 29688–29697.
- (22) Khatal, L.; More, H. Development and Validation of a Liquid Chromatography-Tandem Mass Spectrometry Method for Quantification of Lupeol in Plasma and Its Application to Pharmacokinetic Study in Rats. *J. Chromatogr B Anal Technol. Biomed Life Sci.* **2019**, *1121*, 58–65.
- (23) Hassan, A. R.; Amer, K. F.; El-Toumy, S. A.; Nielsen, J.; Christensen, S. B. A New Flavonol Glycoside and Other Flavonoids from the Aerial Parts of Taverniera Aegyptiaca. *Nat. Prod Res.* **2019**, *33* (8), 1135–1139.
- (24) Abraham, M. J.; Murtola, T.; Schulz, R.; Páll, S.; Smith, J. C.; Hess, B.; Lindahl, E. Gromacs: High Performance Molecular Simulations through Multi-Level Parallelism from Laptops to Supercomputers. *SoftwareX* **2015**, *1–2*, 19–25.
- (25) Tiwari, S.; Shishodia, S. K.; Shankar, J. Docking Analysis of Hexanoic Acid and Quercetin with Seven Domains of Polyketide Synthase A Provided Insight into Quercetin-Mediated Aflatoxin Biosynthesis Inhibition in Aspergillus Flavus. *3 Biotech* **2019**, *9* (4), 149.
- (26) Ghaly, S. M. A.; Khan, M. O. Design, Simulation, Modeling, and Implementation of a Square Helmholtz Coil in Contrast with a Circular Coil for MRI Applications. *Eng. Technol. Appl. Sci. Res.* **2019**, *9* (6), 4990–4995.
- (27) Loske, D. The Impact of COVID-19 on Transport Volume and Freight Capacity Dynamics: An Empirical Analysis in German Food Retail Logistics. *Transp Res. Interdiscip Perspect* **2020**, *6*, 100165.
- (28) Pang, Z.; Chen, J.; Wang, T.; Gao, C.; Li, Z.; Guo, L.; Xu, J.; Cheng, Y. Linking Plant Secondary Metabolites and Plant Microbiomes: A Review. *Frontiers in Plant Science.* **2021**, *12*, 621276.
- (29) Arbain, D.; Saputri, G. A.; Syahputra, G. S.; Widiyastuti, Y.; Susanti, D.; Taher, M. Genus Pterocarpus: A Review of Ethnopharmacology, Phytochemistry, Biological Activities, and Clinical Evidence. *Journal of Ethnopharmacology.* **2021**, *278*, 114316.
- (30) Baharfar, R.; Azimi, R.; Mohseni, M. Antioxidant and Antibacterial Activity of Flavonoid-, Polyphenol- and Anthocyanin-Rich Extracts from Thymus Kotschyannus Boiss & Hohen Aerial Parts. *J. Food Sci. Technol.* **2015**, *52* (10), 6777–6783.
- (31) Aryal, S.; Baniya, M. K.; Danekhu, K.; Kunwar, P.; Gurung, R.; Koirala, N. Total Phenolic Content, Flavonoid Content and Antioxidant Potential of Wild Vegetables from Western Nepal. *Plants* **2019**, *8* (4), 96.
- (32) Saidurrahman, M.; Mujahid, M.; Siddiqui, M. A.; Alsawayt, B.; Rahman, M. A. Evaluation of hepatoprotective activity of ethanolic extract of Pterocarpus marsupium Roxb. leaves against paracetamol-induced liver damage via reduction of oxidative stress. *Phytomedicine Plus* **2022**, *2*, 100311.
- (33) Sarian, M. N.; Ahmed, Q. U.; Mat So'Ad, S. Z.; Alhassan, A. M.; Murugesu, S.; Perumal, V.; Syed Mohamad, S. N. A.; Khatib, A.; Latip, J. Antioxidant and Antidiabetic Effects of Flavonoids: A Structure-Activity Relationship Based Study. *Biomed Res. Int.* **2017**, *8386065*.
- (34) Telagari, M.; Hullatti, K. In-Vitro α -Amylase and α -Glucosidase Inhibitory Activity of Adiantum Caudatum Linn. and Celosia Argentea Linn. Extracts and Fractions. *Indian J. Pharmacol* **2015**, *47* (4), 425–9.
- (35) Aravind, S. R.; Saboo, B.; Sadikot, S.; Shah, S. N.; Makkar, B. M.; Kalra, S.; Kannampilly, J.; Kesavadev, J.; Ghoshal, S.; Zargar, A. H.; Nigam, A.; Hazra, D. K.; Tripathi, K.; Dharmalingam, M.; Shah, P.; Gandhi, P.; Sahay, R.; Unnikrishnan, R.; Gupta, S.; Bajaj, S.; Mukhopadhyay, S.; Kale, S. Consensus Statement on Management of Post-Prandial Hyperglycemia in Clinical Practice in India. *J. Assoc Physicians India* **2015**, *63* (8), 45–58.
- (36) Sun, C.; Zhao, C.; Guven, E. C.; Paoli, P.; Simal-Gandara, J.; Ramkumar, K. M.; Wang, S.; Buleu, F.; Pah, A.; Turi, V.; Damian, G.; Dragan, S.; Tomas, M.; Khan, W.; Wang, M.; Delmas, D.; Portillo, M. P.; Dar, P.; Chen, L.; Xiao, J. Dietary Polyphenols as Antidiabetic Agents: Advances and Opportunities. *Food Front* **2020**, *1* (1), 18–44.
- (37) Dimitriadis, G. D.; Tessari, P.; Go, V. L. W.; Gerich, J. E. α -Glucosidase Inhibition Improves Postprandial Hyperglycemia and Decreases Insulin Requirements in Insulin-Dependent Diabetes Mellitus. *Metabolism* **1985**, *5* (2), 107–111.
- (38) Seema, G.; Gupta, V.; Baljinder, B.; Maithani, M.; Bansal, P.; Gairola, S. Phytochemistry and Pharmacological Activities of Pterocarpus Marsupium- a Review. *Int. Res. J. Pharm.* **2010**, *1* (1), 100–104.
- (39) Fu, M.; Shen, W.; Gao, W.; Namujia, L.; Yang, X.; Cao, J.; Sun, L. Essential Moieties of Myricetins, Quercetins and Catechins for Binding and Inhibitory Activity against α -Glucosidase. *Bioorg Chem.* **2021**, *115*, 105235.
- (40) Choi, C. W.; Choi, Y. H.; Cha, M. R.; Yoo, D. S.; Kim, Y. S.; Yon, G. H.; Hong, K. S.; Kim, Y. H.; Ryu, S. Y. Yeast α -Glucosidase Inhibition by Isoflavones from Plants of Leguminosae as an in Vitro Alternative to Acarbose. *J. Agric. Food Chem.* **2010**, *58*, 9988–9993.
- (41) Smyth, W. F.; Smyth, T. J. P.; Ramachandran, V. N.; O'Donnell, F.; Brooks, P. Dereplication of Phytochemicals in Plants by LC-ESI-MS and ESI-MS N. *TrAC - Trends in Analytical Chemistry.* **2012**, *33*, 46–54.
- (42) Cabezudo, I.; Salazar, M. O.; Ramallo, I. A.; Furlan, R. L. E. Effect-Directed Analysis in Food by Thin-Layer Chromatography Assays. *Food Chem.* **2022**, *390*, 132937.
- (43) Dewanjee, S.; Gangopadhyay, M.; Bhattacharya, N.; Khanra, R.; Dua, T. K. Bioautography and Its Scope in the Field of Natural Product Chemistry. *Journal of Pharmaceutical Analysis* **2015**, *5*, 75–84.
- (44) Singh, P.; Bajpai, V.; Gupta, A.; Gaikwad, A. N.; Maurya, R.; Kumar, B. Identification and Quantification of Secondary Metabolites of Pterocarpus Marsupium by LC-MS Techniques and Its in-Vitro Lipid Lowering Activity. *Ind. Crops Prod* **2019**, *127*, 26–35.
- (45) Veiko, A. G.; Lapshina, E. A.; Zavodnik, I. B. Comparative Analysis of Molecular Properties and Reactions with Oxidants for Quercetin, Catechin, and Naringenin. *Mol. Cell. Biochem.* **2021**, *476*, 4287–4299.
- (46) Khairnar, S.; Pawar, S.; Patil, V.; Rudrapal, M. Effect of Vanillic Acid in Streptozotocin Induced Diabetic Neuropathy. *Asian J. Biol. Life Sci.* **2021**, *9*, 306–312.
- (47) Aryal, B.; Niraula, P.; Khadayat, K.; Adhikari, B.; Khatri Chhetri, D.; Sapkota, B. K.; Bhattarai, B. R.; Aryal, N.; Parajuli, N. Antidiabetic, Antimicrobial, and Molecular Profiling of Selected Medicinal Plants. *Evidence-based Complement Altern Med.* **2021**, *3*, 5510099.
- (48) Aleixandre, A.; Gil, J. V.; Sineiro, J.; Rosell, C. M. Understanding Phenolic Acids Inhibition of α -Amylase and α -Glucosidase and Influence of Reaction Conditions. *Food Chem.* **2022**, *372*, 131231.
- (49) Vinothiya, K.; Ashokkumar, N. Modulatory Effect of Vanillic Acid on Antioxidant Status in High Fat Diet-Induced Changes in Diabetic Hypertensive Rats. *Biomed Pharmacother* **2017**, *87*, 640–652.
- (50) Sun, H.; Liu, X.; Long, S. R.; Teng, w.; Ge, H.; Wang, Y.; Yu, S.; Xue, Y.; Zhang, Y.; Li, X.; Li, W. Antidiabetic Effects of Pterostilbene through PI3K/Akt Signal Pathway in High Fat Diet and STZ-Induced Diabetic Rats. *Eur. J. Pharmacol.* **2019**, *859*, 172526.
- (51) Bone, A. J.; Hii, C. S. T.; Brown, D.; Smith, W.; Howell, S. L. Assessment of the Antidiabetic Activity of Epicatechin in Streptozotocin-Diabetic and Spontaneously Diabetic BB/E Rats. *Biosci Rep* **1985**, *5*, 215–221.

- (52) Den Hartogh, D. J.; Gabriel, A.; Tsiani, E. Antidiabetic Properties of Curcumin Ii: Evidence from in Vivo Studies. *Nutrients* **2020**, *12* (1), 58.
- (53) Mirmiranpour, H.; Khaghani, S.; Zandieh, A.; Khalilzadeh, O.; Gerayesh-Nejad, S.; Morteza, A.; Esteghamati, A. Amygdalin Inhibits Angiogenesis in the Cultured Endothelial Cells of Diabetic Rats. *Indian J. Pathol Microbiol* **2012**, *55* (2), 211–4.
- (54) Bule, M.; Abdurahman, A.; Nikfar, S.; Abdollahi, M.; Amini, M. Antidiabetic Effect of Quercetin: A Systematic Review and Meta-Analysis of Animal Studies. *Food Chem. Toxicol.* **2019**, *125*, 494–502.
- (55) Gaur, R.; Yadav, K. S.; Verma, R. K.; Yadav, N. P.; Bhakuni, R. S. In Vivo Anti-Diabetic Activity of Derivatives of Isoliquiritigenin and Liquiritigenin. *Phytomedicine* **2014**, *21* (4), 415–22.
- (56) Li, S.; Zhang, Y.; Sun, Y.; Zhang, G.; Bai, J.; Guo, J.; Su, X.; Du, H.; Cao, X.; Yang, J.; Wang, T. Naringenin Improves Insulin Sensitivity in Gestational Diabetes Mellitus Mice through AMPK. *Nutr Diabetes* **2019**, *9* (1), 28.
- (57) De Sousa, E.; Zanatta, L.; Seifriz, I.; Creczynski-Pasa, T. B.; Pizzolatti, M. G.; Szpoganicz, B.; Barreto Silva, F. R. M. Hypoglycemic Effect and Antioxidant Potential of Kaempferol-3,7-O-(α)-Dirhamnoside from Bauhinia Forficata Leaves. *J. Nat. Prod* **2004**, *67* (5), 829–832.
- (58) Gupta, R.; Sharma, A. K.; Sharma, M. C.; Dobhal, M. P.; Gupta, R. S. Evaluation of Antidiabetic and Antioxidant Potential of Lupeol in Experimental Hyperglycaemia. *Nat. Prod Res.* **2012**, *26*, 1125–1129.
- (59) Wolfram, S.; Raederstorff, D.; Preller, M.; Wang, Y.; Teixeira, S. R.; Riegger, C.; Weber, P. Epigallocatechin Gallate Supplementation Alleviates Diabetes in Rodents. *J. Nutr.* **2006**, *136*, 2512.
- (60) Tvrdá, E.; Straka, P.; Galbavy, D.; Ivanic, P. Epicatechin Provides Antioxidant Protection to Bovine Spermatozoa Subjected to Induced Oxidative Stress. *Molecules* **2019**, *24* (18), 3226.
- (61) Chakravarthy, B. K.; Gode, K. D. Isolation of (–)-Epicatechin from Pterocarpus Marsupium and Its Pharmacological Actions. *Planta Med.* **1985**, *51*, 56–59.
- (62) Elango, B.; Dornadula, S.; Paulmurugan, R.; Ramkumar, K. M. Pterostilbene Ameliorates Streptozotocin-Induced Diabetes through Enhancing Antioxidant Signaling Pathways Mediated by Nrf2. *Chem. Res. Toxicol.* **2016**, *29* (1), 47–57.
- (63) Krishnaveni, K. S.; Srinivasa Rao, J. V. An Isoflavone from Pterocarpus Santalinus. *Phytochemistry* **2000**, *53*, 605–606.
- (64) Beg, A.; Khan, F. I.; Lobb, K. A.; Islam, A.; Ahmad, F.; Hassan, M. I. High Throughput Screening, Docking, and Molecular Dynamics Studies to Identify Potential Inhibitors of Human Calcium/calmodulin-Dependent Protein Kinase IV. *J. Biomol Struct Dyn* **2019**, *37* (8), 2179–2192.
- (65) Abdelsalam, S. S.; Korashy, H. M.; Zeidan, A.; Agouni, A. The Role of Protein Tyrosine Phosphatase (PTP)-1B in Cardiovascular Disease and Its Interplay with Insulin Resistance. *Biomolecules.* **2019**, *9* (7), 286.
- (66) Kuzmanic, A.; Zagrovic, B. Determination of Ensemble-Average Pairwise Root Mean-Square Deviation from Experimental B-Factors. *Biophys. J.* **2010**, *98* (5), 861–871.
- (67) Rodier, F.; Bahadur, R. P.; Chakrabarti, P.; Janin, J. Hydration of Protein-Protein Interfaces. *Proteins Struct Funct Genet* **2005**, *60* (1), 36–45.
- (68) Bhardwaj, V. K.; Singh, R.; Sharma, J.; Rajendran, V.; Purohit, R.; Kumar, S. Identification of Bioactive Molecules from Tea Plant as SARS-CoV-2 Main Protease Inhibitors. *J. Biomol Struct Dyn* **2021**, *39*, 3449–3458.
- (69) Eleftheriou, P.; Geronikaki, A.; Petrou, A. PTP1b Inhibition, A Promising Approach for the Treatment of Diabetes Type II. *Curr. Top Med. Chem.* **2019**, *19*, 246–263.